RESEARCH PAPER
https://doi.org/10.1071/WF22062

International Journal of WILDLAND FIRE
International Association of Wildland Fire

Calculating fire danger of cured grasslands in temperate climates – the elements of the Grassland Fire Index (GLFI)

K.-P. Wittich[A], C. Böttcher[A,*], P. Stammer[A] and M. Herbst[A]

For full list of author affiliations and declarations see end of paper

*Correspondence to:
C. Böttcher
Deutscher Wetterdienst (German Meteorological Service), Centre for Agrometeorological Research, Bundesallee 33, D-38116 Braunschweig, Germany
Email: christopher.boettcher@dwd.de

ABSTRACT

Background. Increasing extreme weather events due to climate change require updated environmental monitoring and prediction systems in Germany. **Aim.** The Grassland Fire Index (GLFI), developed by the German Meteorological Service ~15 years ago for temperate climates, was revised to improve fire-danger predictions during the fire season. Our paper gives insight into the new model version. **Methods.** The former fire-behaviour core, i.e. Fosberg's Fire Weather Index (FWI), is replaced by the standardised fire-reaction intensity, a different fuel-moisture of extinction term, and a replica of the fire-spread rate of the Canadian FFBP-System. A standardised ease-of-ignition index is added as a measure of ignition success. The fire module is supplied with diurnal dead-grass fuel-moisture calculations based on the water-budget and energy-balance concept. **Key results.** The GLFI output is compared with diurnal fuel-moisture measurements and results of Wotton's Grass-Fuel-Moisture model, Fosberg's FWI, and Cheney's rate of spread equation. The GLFI computes periods with a high fuel moisture more realistically, whereas it exceeds Cheney's rate-of-fire spread systematically at lower wind speeds, which leads to higher danger ratings during calm-air conditions (as requested by users). **Conclusions and Implications.** The GLFI estimates dead-fuel moisture and fire danger on open, horizontal topography according to the current scientific level. Model extensions are necessary to run the model on complex topography under varying greenness and occasional frost conditions.

Keywords: field and laboratory measurements, fire behaviour, fire intensity, fuel moisture, hourly fire-danger rating, ignition index, rate of spread, theoretical model.

Received: 4 May 2022
Accepted: 25 June 2023
Published: 19 July 2023

Cite this:
Wittich K-P *et al.* (2023)
International Journal of Wildland Fire
32(8), 1212–1225. doi:10.1071/WF22062

Introduction

Characterised by 0.3–3 h time-lags, cured grasses belong to the light fuel types whose moisture content adapts quickly to variable meteorological conditions (Anderson 1990*b*; Catchpole *et al.* 2001; Marsden-Smedley and Catchpole 2001; Wotton 2009). After rain showers and dew-forming nights, short spells of fine and windy weather are sufficient to dry cured grasses out. When their moisture content falls below approximately 30% (dry-weight basis), they become readily ignitable (Albini 1976; Cheney and Sullivan 1997).

According to dry/wet-spell lengths analyses covering the years 1960–2010, western Central Europe (incl. Germany) showed no dominance of dry weather conditions in contrast to southern and eastern Europe (Zolina *et al.* 2013) and wildland-fire prone regions worldwide (Breinl *et al.* 2020). The temperate and semi-humid climate is the main reason why Germany was less vulnerable to wildfires in the past (see also Dawson and Goldsmith (2018) for the world map of annual number of wet days ($\geq$0.1 mm/day)). Nevertheless, nation-wide climate-change analyses and projections using the Canadian Fire Weather Index show that weather conditions are becoming more favourable for wildfires (Deutscher Wetterdienst 2022).

In order to develop appropriate fire preparedness and response strategies for upcoming spells of fire weather, fire managers need weather-based wildfire-danger predictions. The term 'fire danger' used here follows the definition of NOAA-National Weather Service

(2023), meaning 'a subjective expression of an objective assessment of environmental (fuels and weather) factors which influence whether fires will start and how they might spread'.

Socioeconomic and environmental sectors benefit from grassland fire-danger ratings (e.g. Müller 1992). For example, fire-danger forecasts are relevant for the time management of cereal crop harvesting. To avoid crop fires caused by harvesting operations during the hot and dry midday hours (as a result of overheated machine parts or spark emissions), field work should be pre- or postponed to the cooler morning or evening hours when there is a lower fire danger. Similarly, high-speed grinding trains that are used for railroad track maintenance should defer their spark-emitting grinding operations to the dew-forming night hours or rainy days. Other restrictions apply to the operation of vintage steam train rides to prevent fires on embankments caused by ejected embers, and the conducting of firearm exercises by armed forces if the danger rating is high. Furthermore, economic damages due to careless lighting of fires by humans can be reduced by issuing public fire-weather forecasts through the electronic and classic media for days with high fire danger.

Due to this scope of applications, our updated fire-danger index for grass-covered areas in Germany should:

- Respond to weather conditions throughout the diurnal cycle during the summer half-year;
- Be easy enough to run in an operational mode for about 500 stations; and
- Follow the current state of scientific knowledge.

The GLFI's predecessor version

The GLFI's predecessor (in operation since 2005, but unpublished) was based on Fosberg's (1978) hourly Fire Weather Index (FWI) designed for regional climate conditions in the United States. The FWI includes Rothermel's (1972) rate-of-spread component and an energy-release (flame-length) formula. Fuel moisture was estimated by the equilibrium value F_{eq} in the range 0–30% (dry-weight basis, 30% representing the fibre-saturation point, FSP, and moisture of extinction, F_{ex}). Thus, data input could be reduced to relative humidity, air temperature, and wind speed. For situations with variable weather (which are typical in Western Europe); however, we found that these three parameters are inadequate to capture the diurnal danger level correctly when the canopy is wet but screen-height relative humidity stays below 100%, resulting in $F_{eq} < 30\%$ and FWI > 0 (scale: 0–100). To avoid misinterpretations caused by the FWI's non-cumulative nature (no memory and time-lag effect), its F_{eq} scheme was replaced by a dead-grass moisture model similar to that described below. Finally, the hourly FWI was combined with DWD's dead-grass moisture index to get higher ratings under calm–dry weather conditions.

Materials and methods

The new version of the GLFI is an upgrade of the hybrid index above. In the following sections, we describe the current fuel-moisture core and the coupled fire-behaviour module that is similar to that used in the national fire-danger rating systems of the major wildfire countries – Australia (McArthur 1966; Matthews 2022), Canada (Forestry Canada Fire Danger Group 1992), and the United States (National Wildfire Coordinating Group 2002). An *ad hoc* crop-fire experiment, grass-moisture measurements and a comparison with Fosberg's FWI and Wotton's (2009) Grass-Fuel Moisture (GFM) model complete this article.

Model description

Formulas describing the energy balance and the water budget provide the basics for calculating the moisture content of a fully cured, dead grass canopy. The complex canopy structure is treated as a single layer following the so-called 'big-leaf concept' (Monteith 1965), which scales the vertical leaf-area density profile and energy-flux distribution down to a representative 'source-sink' fuel-bed level (thus avoiding more complex and time-consuming multi-layer modelling, e.g. Thompson (1981) and Matthews (2006)). Four processes of water exchange between the fuel bed and the ambient air are regarded: water-vapour ad- and desorption, absorption of intercepted rain and dew water and evaporation. Uptake of soil water by dead grass is excluded.

The model assumes that the terrain is covered by continuous grass fuel whose load and structure are invariable over space and time. Relief parameters, such as the surface azimuth and slope angle, are not considered, although they affect fire behaviour (Sharples 2009).

The GLFI uses an hourly time step to track the diurnal cycle of fire danger, which usually peaks in the afternoon when wind speed and gustiness are maximum and atmospheric humidity and fuel moisture are minimum (Beck *et al.* 2002; Lex and Wittich 2002), and to flag fire-prone nights when fuel moisture remains at a low level, e.g. during drought periods, prolonged heatwaves, and foehn events.

Fuel moisture descriptors

Fuel moisture content, F, is defined as the ratio of the mass of water contained in a fuel sample, m_w, to its dry mass, m_d, obtained after oven drying at 105°C (National Wildfire Coordinating Group 2008; Matthews 2010):

$$F = \frac{m_w}{m_d} = \frac{m_t - m_d}{m_d} \quad (1)$$

where $m_t = m_w + m_d$ is the total fuel loading, i.e. the mass of undried dead leaves per unit ground area (in $kg\,m^{-2}$). The standard dry-mass value used in the GLFI is $m_d = 0.65$ $kg\,m^{-2}$, which is in the range of typical grassland fuels

(0.2–0.7 kg m^{-2}, Anderson 1982; Forestry Canada Fire Danger Group 1992; Cruz *et al.* 2020) while tallgrass communities may reach maximum m_d values of up to 1.5 kg m^{-2} (Kidnie and Wotton 2015).

The mass of water in a fuel sample, m_w, splits into external water, m_e, held on the leaf surface, and internal water, m_i, enclosed in the cell cavities and walls, i.e. $m_w = m_e + m_i$. During rain and dew periods, external water accumulates on the leaves until the interception storage capacity, $m_{e,max}$, is reached, written as:

$$m_{e,\,max} = \rho_w (a_1 + a_2 m_d) 10^{-3} \quad (2a)$$

with ρ_w the density of water ($=10^3$ kg m^{-3}) and $a_{1,2}$ fuel-specific parameters proposed by Putuhena and Cordery (1996) for tussock grasses, i.e. $a_1 = 0.069$ mm, $a_2 = 0.510$ mm (kg m^{-2})$^{-1}$ derived from laboratory rain experiments. Alternatively, $m_{e,max}$ (in kg m^{-2}) can be related to the leaf-area index, LAI (in m^2 m^{-2}), according to the empirical relationship of Menzel (1997), i.e.

$$m_{e,\,max} = a \log_{10}(1 + \mathrm{LAI}) \quad (2b)$$

with $a = 1.2$ for grassland (Vegas Galdos *et al.* 2012).

The maximum of internal water can be easily estimated using:

$$m_{i,\,max} = m_d F_{max} - m_{e,\,max} \quad (3)$$

Dead grass maximum fuel moisture is in the range of F_{max} = 200–450% (Couturier and Ripley 1973; de Groot *et al.* 2005). In the GLFI, the fuel-moisture maximum is set at 250% (Forestry Canada Fire Danger Group 1992; Wotton 2009).

The m_i-moisture regime is divided by the fibre-saturation point into two sub-regimes where internal water moves as free water (FSP $< F < m_{i,max}/m_d$) and where it is bound to cell-wall structures and shows hygroscopic behaviour ($0 < F \leq$ FSP). The dynamic approach FSP $= F_{eq,max} \sim F_{eq}$ ($h_{i,sat}$,T_i) is used, where $h_{i,sat}$ is the intra-leaf relative humidity near saturation ($=0.95$), T_i the intra-leaf temperature, and F_{eq} is evaluated by Anderson (1990*a*) under constant climate-chamber conditions at the end of ad-/desorption processes. Cheatgrass-based parameter settings (quadratic in T; see his table 3) hold for intra-leaf temperatures between 5 and 45°C, making the F_{eq}-relationship suitable for operational use under a variety of atmospheric conditions. Fig. 1 shows a comparison between the FSPs of Anderson (1990*a*) and Van Wagner (1972), whose F_{eq} formula (calibrated for reed grass at 26.7°C, with linear corrections over the range 15.6–48.9°C) was used by Wotton (2009) in his GFM model. The FSP profiles deviate from each other at the cold and warm ends of the temperature range. The insets demonstrate the robustness of both formulas to reproduce fictive drying-chamber conditions.

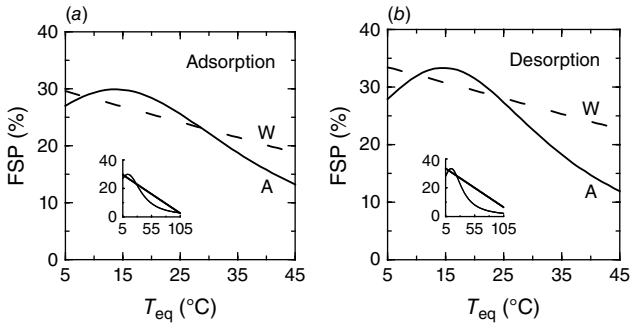

Fig. 1. Fibre-saturation point (FSP) for different equilibrium temperatures and fixed relative humidity of 95% according to formulas provided by Van Wagner (1972) and Wotton (2009, dashed line marked by 'W') and Anderson (1990*a*, solid curve marked by 'A') using parameters for (*a*) adsorption and (*b*) desorption. The inlays show the hypothetical FSP(T_{eq}) relationship with temperature extrapolated to the standard laboratory drying temperature of 105°C, where plant materials become kiln dry. Note that the range of validity of F_{eq}-based FSP only extends to $T_{eq} \cong 45$°C, so the extreme range beyond this has to be interpreted with caution.

Energy balance of the grass layer

Moisture content of dead grass canopies depends on water-budget and energy-balance principles (Monteith 1965; Thompson 1981) that are interconnected via the latent heat-flux density λE (in W m^{-2}):

$$\lambda E = -\frac{\rho_a \lambda \{q_a - h_i q_{sat}(T_i)\}}{r_a + r_c} \quad (4)$$

with λ the latent heat of vaporisation of water ($=2.5 \times 10^6$ J kg^{-1}), E (in kg m^{-2} s^{-1}) the mass flux of water vapour between the grass layer and the ambient air (positive upward), ρ_a the density of air ($=1.2$ kg m^{-3}, subscript 'a' for air), q_a (in kg kg^{-1}) the specific humidity at screen height z (2 m), $q_{sat}(T_i)$ the temperature-dependent intra-leaf saturation value of q, and h_i and T_i the intra-leaf fractional relative humidity and temperature (in K). Canopy and aerodynamic resistances, r_c and r_a (in s m^{-1}), have to be overcome by water vapour along its diffusion path from the leaf's cell structure to the canopy (i.e. big-leaf) surface, and from the canopy towards screen-height level.

The intra-leaf temperature is approximated by the canopy temperature, T_c (subscript c for canopy), as follows:

$$T_c = T_a + \frac{(1-\beta)R_{net,iso} + \frac{\rho_a \lambda}{r_a + r_c}[q_a - h_i q_{sat}(T_a)]}{(1-\beta)4\varepsilon\sigma T_a^3 + \frac{\rho_a c_p}{r_a} + \frac{\rho_a \lambda}{r_a + r_c} h_i \frac{\partial q_{sat}}{\partial T}(T_a)} \quad (5)$$

with T_a (in K) the air temperature at screen height, β a proportionality factor (0.4, suitable for model calibration) that coarsely represents the temperature and moisture conditions in the upper soil, $R_{net,iso}$ the isothermal net radiant flux density (in W m^{-2}), ε the emissivity of the fuel bed

(0.966, Sutherland 1986), σ the Stefan-Boltzmann constant (5.67×10^{-8} W m^{-2} K^{-4}), c_p the specific heat of air at constant pressure (1005 J kg^{-1} K^{-1}), and $\partial q_{sat}(T)/\partial T$ the derivative of $q_{sat}(T)$ taken at T_a. The isothermal net radiation reads:

$$R_{net,iso} = (1 - \alpha)S_{\downarrow} + \varepsilon L_{\downarrow} - \varepsilon\sigma T_a^4 \quad (6)$$

with α the albedo (0.27), and $L_{\downarrow}$, $S_{\downarrow}$ the downwelling long- and shortwave radiation flux densities.

The aerodynamic resistance, r_a, expresses the efficiency of turbulence on the vertical momentum and energy transfer between source-sink height $z_0 + d$ and screen height z, with d the displacement height and z_0 the roughness length of the canopy. Both parameters depend on the height of the canopy, z_c (in m), i.e. $z_0 \approx 0.1 \times z_c$ and $d \approx 2/3 \times z_c$ (Campbell 1977; $z_c = 0.25$ m used as default in the GLFI). The resistance (Choudhury *et al.* 1986) reads:

$$r_a = \left\{ \frac{\ln\left(\frac{z-d}{z_0}\right)}{\kappa} \right\}^2 \frac{(1 - 5 \times Ri_b)^{\delta}}{u_z} \quad (7)$$

with κ (0.4) the von Karman constant, Ri_b the bulk-Richardson number, δ a stability-dependent exponent (-2.0 for $Ri_b > 0$, -0.75 for $Ri_b < 0$), and u_z the wind speed (in m s^{-1}) at screen height. The Ri_b number considers the effect of diabatic lapse rate:

$$Ri_b = g(z - d)(T_a - T_c)/(T_a u_z^2) \quad (8)$$

where g is the acceleration due to gravity (9.81 m s^{-2}).

In order to estimate the relative humidity at the liquid-vapour interface in the cavities of the grass leaves, h_i, we use the approximation (e.g. Nelson 1983):

$$h_i \approx h_{eq} = \exp\left(\frac{\Psi_{eq} M}{R^* \times T_{eq}}\right) \quad (9)$$

with h_{eq} the equilibrium humidity, M the molecular weight of water (18.015 kg mol^{-1}), R^* the universal gas constant (8.314 J mol^{-1} K^{-1}), T_{eq} the equilibrium leaf temperature (approximated by T_c), and Ψ_{eq} the water potential (in m^2 s^{-2} = J kg^{-1}) given by Gibbs free energy described by the numerical value equation:

$$\Psi_{eq} = -\exp(c_1 + c_2 F_{eq}) \quad (10)$$

with F_{eq} approximated by m_i/m_d, and $c_{1,2}$ cheatgrass-specific constants according to Anderson (1990*a*), which take hysteresis between ad- and desorption into account. Cheatgrass can be found on nutrient-poor sandy soils in Germany and on coarsely granular structured or crushed-rock substrates along road sides and railway track beds.

In Eqn 5, both r_a and h_i include the canopy temperature. To avoid recursive iterations in T_c to fulfil the energy-balance equation, we estimate T_c for use in Eqns 8, 9 by the mean-value theorem:

$$T_c(t) = T_c(t - \Delta t) + \{\partial T_c/\partial T_a\}\{T_a(t) - T_a(t - \Delta t)\} \quad (11)$$

with t the time (in s), Δt the hourly time step (= 3600 s), and $\partial T_c/\partial T_a$ a temperature ratio set to 1.2 to allow for the larger diurnal amplitude at fuel-bed level compared to the smaller one at 2 m.

The internal canopy resistance r_c is parameterised by:

$$r_c = r_{c,max}\left(\frac{r_{c,res}}{r_{c,max}}\right)^{m_i/m_{i,max}} \quad (12)$$

with $r_{c,res}$ (10–40 s m^{-1}) the residual vapour resistance at the wet end of internal moisture range where $m_i = m_{i,max}$, and $r_{c,max}$ the maximum resistance at the dry end where $m_i = 0$. Here, we set $r_{c,max} = 4000 \times (m_{d,ref}/m_d)^a$ with $a \geq 1$ and $m_{d,ref} = 0.65$ kg m^{-2} (see Thompson (1981) and Alfieri *et al.* (2008) for similar r_c value range). Our $r_{c,max}$ approximation assumes that m_d is proportional to the evaporating leaf surface (or LAI), and the larger the leaf surface, the smaller the canopy resistance to water-vapour losses.

To demonstrate the interrelation between the temporal behaviour of fuel moisture and r_c, the moisture exponent of Eqn 12 is replaced by the exponential drying relationship $m_i = m_{i,max} \times \exp(-t/\tau)$, using $\tau = (m_d/\rho_b)^2/D$ the time-lag (in s) with ρ_b the bulk density arbitrarily set at 2.6 kg m^{-3} and D the diffusion coefficient of the order 1×10^{-5} m^2 s^{-1}. Fig. 2 exemplifies the temporal fuel-moisture curves for the three settings $m_d = 0.325$, 0.65 and 1.3 kg m^{-2}, starting with $F_{max} = m_{i,max}/m_d = 100\%$ at time $t = 0$. The larger the fuel load, the slower the decrease of F due to higher time-lags. The r_c profiles start with $r_{c,ref} = 10$ s m^{-1}, and at the end of drying they are at their maximum values between 8000 and 1000 s m^{-1}.

In the current version of the GLFI, the canopy resistance remains unaffected by the vapour-exchange direction in the

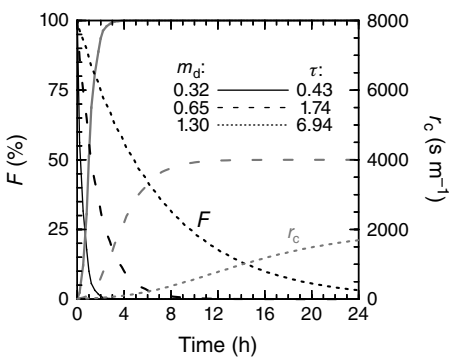

Fig. 2. Decreasing fuel moisture with time, F (black curves), and corresponding canopy resistance, r_c (grey curves) for different fuel-bed characteristics m_d (in kg m^{-2}) and τ (in h), see text; $r_{c,max}$ parameter: $a = 1$, canopy height: $z_c = \{0.12, 0.25, 0.5\}$ m for $m_d = \{0.325, 0.65, 1.3\}$ kg m^{-2}.

hygroscopic moisture range, i.e. $r_{c,des} = r_{c,ads} = r_c$. This is in line with Anderson (1990*b*) and Wotton (2009), who mentioned that the time-lags along opposite ad- and desorption pathways do not differ significantly for cheatgrass ($\tau_{des} = 0.85$ h, $\tau_{ads} = 0.8$ h), but contradictory to Luke and McArthur (1978), who state that desorption should proceed faster than adsorption, i.e. $E_{des} > |E_{ads}|$ and therefore $r_{c,des} \neq r_{c,ads}$.

Water budget of grass fuels

Besides E (Eqn 4), the water-budget equation for the mass of leaf water per unit ground area, m_w, includes the mass fluxes of precipitation and drainage, P and Dr (each in kg m^{-2} s^{-1}), i.e.

$$\frac{\partial m_w}{\partial t} = P - \mathrm{Dr} - E \tag{13}$$

with E split into the contributions of ex- and internal water, $E = E_e + E_i$. The rate of mass change of intercepted *external* water is calculated by:

$$\frac{\partial m_e}{\partial t} = P - \mathrm{Dr} - E_e - A \tag{14}$$

with $E_e > 0$ for evaporation (Eqns 4, 5 with $h_i = 1$ and $0 \le r_c \le r_{c,res}$) and $E_e < 0$ for dewfall, which is a top-down vapour transfer process from ambient air to cool wet leaf surfaces ($h_i = 1$ and $r_c = 0$). As soon as m_e surpasses the interception capacity $m_{e,max}$ because of rain- or dewfall, drainage occurs ($\mathrm{Dr} = m_e - m_{e,max} > 0$, $\mathrm{Dr} = 0$ otherwise).

As long as leaf surfaces are wet ($m_e > 0$), E_e is active but evaporation of *internal* water is inhibited ($E_i = 0$). Nevertheless, m_i can increase up to $m_{i,max}$ as a result of water absorption according to:

$$\frac{\partial m_i}{\partial t} = A - E_i \tag{15}$$

with A the rate at which external water is transferred into internal water (in kg m^{-2} s^{-1}). The process of absorption is assumed to be proportional to the difference between maximum and current intra-leaf water content. Because absorption depends on the physiological characteristics of leaves, a time-scale parameter, τ_{abs} (in s), is incorporated whereby:

$$A = \frac{m_{i,\,max} - m_i}{\tau_{abs}} \tag{16}$$

Here, we assume $\tau_{abs} = 2$–5 h. Laboratory water-absorption experiments by Liang *et al.* (2009) on three different species of fully grown turf grasses resulted in $\tau_{abs} \cong 0.5$–1 h, and McGechan and Pitt (1990) found $\tau_{abs} \cong 15$ h for grass swaths.

Wotton's Grass Fuel Moisture (GFM) model

Wotton's (2009) GFM model, developed as a supplement to the forest-floor related Fine Fuel Moisture Code (FFMC) of the Canadian Forest Fire Danger Rating System, is one of the most advanced mechanistic models concerning diurnal dead grass-moisture variability. It is adapted to fully cured, matted late-winter/early-spring grasses on open unshaded areas and uses hourly input data similar to ours, with the exception of longwave radiation. The theoretical framework of the GFM model complies with the FFMC, e.g. using *e*-folding response times to reach moisture equilibrium and using comparable structural forms of the F_{eq} equation. Processes of energy and water transfer between fuel and atmosphere are thus a little more simplified compared with meteorological approaches described above.

Fire-behaviour prediction module

Besides fuel moisture, the following dynamic fire behavioural traits are included in the GLFI: rate of spread (ros), fire intensity, and an ease-of-ignition index.

Fire-spread rate

According to Forestry Canada Fire Danger Group (1992), rate of forward spread, ros (in m s^{-1}), is given by:

$$\mathrm{ros} = \mathrm{ros}_{max}\{1 - \exp(-b \times f_{F,u})\}^c \tag{17a}$$

with ros_{max} the maximum rate of spread at the end of the fire-growth phase, and b, c empirical coefficients, all three fitted to Australian grass fire data. Each parameter represents two types of fuel-bed characteristics, i.e. mat-forming grass in early spring which has been pressed down by recent winter snowpack, and standing (and better aerated) grass in the summer to autumn season (Table 1 for values currently implemented in the GLFI, but note that higher spread rates are observed in the field, e.g. 6.4 m s^{-1}; see Noble (1991) and listings in Cheney *et al.* (1998) and Cruz *et al.* (2022)).

In Eqn 17a, $f_{F,u}$ is a dimensionless wind-speed and fuel-moisture function that, as an alternative to the original Initial-Spread Index (ISI) of the Canadian Forest Fire Behaviour Prediction System (CFFBPS), is written as:

$$f_{F,u} = \frac{c_1 \times \exp(u_{10}/u_c)}{(c_2 + F)^5} \cong \mathrm{ISI} \tag{17b}$$

with F the fractional fuel moisture content, u_{10} the wind speed measured at 10 m (in m s^{-1}), u_c a wind speed normalisation factor ($= 5.5$ m s^{-1}), and $c_1 = 0.0581$, $c_2 = 0.31$ dimensionless parameters, which, in the range of u_{10} up to 10 m s^{-1}, are fitted to the original ISI formula for fully cured grass (no ground slope) (see Forestry Canada Fire Danger

Table 1. Parameter settings in Eqn 17a for early spring matted grass and late summer standing grass (Forestry Canada Fire Danger Group 1992).

Grass layer	ros_{max} (m s^{-1})	b	c
Matted	3.167	0.031	1.4
Standing	4.167	0.035	1.7

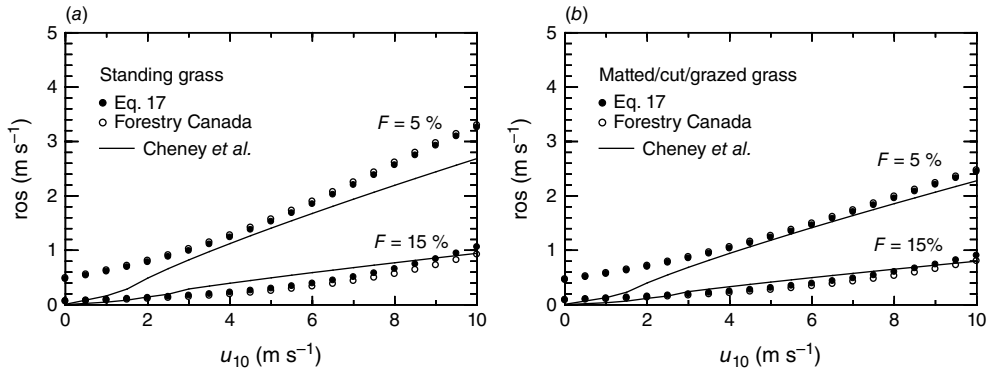

Fig. 3. Rate of spread (ros) as a function of 10 m wind speed based on the relationship of Cheney *et al.* (1998, solid line), Eqn 17 (black dots), and the original formula for fully cured grass provided by the Forestry Canada Fire Danger Group (1992, open circles). The curves represent (*a*) standing undisturbed grass and (*b*) matted and cut or grazed grass. Two moisture regimes are considered: dry (F = 5%) and medium (F = 15%). The F = 25% moisture regime is ignored because fires do not spread after Cheney *et al.* (1998) and are slower than 0.3 m s^{-1} for wind speeds up to u_{10} = 10 m s^{-1} (Forestry Canada Fire Danger Group (1992) and Eqn 17).

Group 1992). High wind speeds and small fuel moistures result in rapid convergence towards ros_{max} via large $f_{F,u}$.

Fig. 3 compares Eqn 17 with the original formula of the CFFBP-System (Forestry Canada Fire Danger Group 1992) and the findings of Cheney *et al.* (1998). As expected, at wind speeds up to u_{10} = 10 m s^{-1}, there is no bias larger than 0.1 m s^{-1} between the original Canadian ros-version and our approximation (white and black circles). However, both formulas (CFFBPS and Eqn 17) overestimate Cheney's ros-values by 0.5 m s^{-1} in the case of standing grass, still air, and low fuel moisture (F = 5%), and by 0.6 m s^{-1} at high wind speeds of 10 m s^{-1}. At medium wind speeds of 5 m s^{-1}, overrating is by about 0.15 m s^{-1}. CFFBPS and Eqn 17 formulas reach their ros_{max} limit at about u_{10} = 17 m s^{-1} (not shown). At this u_{10} value, Cheney's model provides nearly the same propagation speed, but continues to increase under the influence of gale-force winds. The curves plotted for F = 15% show smaller offsets at both ends of the wind speed range, whereas at moderate winds Cheney's ros curve is underrated by up to 0.25 m s^{-1}. At F = 25%, fires do not spread according to Cheney's model (because of a ros-terminating F_{ex} threshold) whereas both the CFFBPS- and Eqn 17-formulas provide an increase in ros from 0.03 to 0.25 m s^{-1} for rising u_{10} from 0 to 10 m s^{-1}. A better conformity between the ros formulas is found for matted fuel beds.

According to Cheney *et al.* (1998), no matter how low the fuel moisture is, the fire front does not propagate when mean wind speed zeros. In contrast, the CFFBP System and Eqn 17 provide rather high ros values (0.5–1 m s^{-1}) if $F \leq$ 5% in still air (see Discussion).

Fuel moisture of extinction

The moisture of extinction, F_{ex}, defines the moisture threshold above which fires will not spread (National Wildfire Coordinating Group 2002) or barely continue to burn (Wilson 1985), and, as a consequence, fuels will hardly ignite (Cheney 1981; Chuvieco *et al.* 2004; Dimitrakopoulos *et al.* 2010).

To estimate F_{ex}, the rearranged form of Eqn 17 can be used assuming that ros = ros_{ex} at $F = F_{ex}$, i.e.

$$F_{ex} = \left(-b\frac{c_1 \times \exp(u_{10}/u_c)}{\ln\{1-(ros_{ex}/ros_{max})^{1/c}\}}\right)^{1/5} - c_2 \qquad (18)$$

Because ros_{ex} in the denominator disallows zeroing, we assume that ros_{ex}/ros_{max} is in the order of 10^{-3}, i.e. fire line propagates over a distance of 11.4 and 15.0 m h^{-1} on matted and standing grass areas, respectively. In still air, F_{ex} = 34% (45%) in standing (matted) grass and rises with increasing wind speed.

Fire intensity

Fire-reaction intensity, I, defined as the energy release per unit burning area at the front of a spreading fire (in W m^{-2}, Sneeuwjagt and Frandsen 1977; Cheney 1990; Wilson 1990), is written as:

$$I = H_{fc}\frac{\partial w}{\partial t} = H_{fc}\frac{\partial w}{\partial x}\frac{\partial x}{\partial t} = H_{fc}\frac{\Delta w}{\Delta x}\text{ros} \qquad (19)$$

with H_{fc} the heat released from fuel combustion (14 000–19 000 kJ kg^{-1} for different grass species and moisture contents (Luke and McArthur 1978; Cheney and Sullivan 1997; Kidnie and Wotton 2015), $\partial w/\partial t$ (with a positive sign) the loss rate of fuel mass per unit ground area of the combustion zone, Δw (in kg m^{-2}) the net weight of combustible fuel per unit ground area, and Δt (in s) the residence time. During the time increment Δt, the fire front with its rate of forward spread, ros (in m s^{-1}), has passed

the cross-frontal distance Δx (in m) represented by the horizontal flame depth that extends 'from the leading edge of the flame front to the rear edge of the flaming area' where combustion is still active (Alexander 1982). Thus, smouldering combustion behind the flaming area remains disregarded.

The net amount of fuel consumed by the fire depends on the moisture content as follows:

$$\Delta w = m_{\mathrm{d}} \times \min\left[\max\left\{\frac{F_{\mathrm{ex}} - F}{F_{\mathrm{ex}} - F_{\mathrm{low}}}, 0\right\}, 1\right] \qquad (20)$$

with F_{ex} defined by Eqn 18, and $F_{\mathrm{low}} = 6\%$ the setting below which combustion is nearly complete (Cheney 1981). Consequently, Δw ranges from 0 to m_{d}.

The GLFI is given by the dimensionless [0–1]-ratio:

$$\frac{I}{I_{\max}} = \frac{\Delta w}{m_{\mathrm{d}}} \times \frac{\mathrm{ros}}{\mathrm{ros}_{\max}} \times \left(\frac{\Delta x}{\Delta x_{\max}}\right)^{-1} \qquad (21)$$

Taking $\Delta x/\Delta x_{\max} = 1$ leads to $I/I_{\max} = (\Delta w \times \mathrm{ros})/(\Delta w \times \mathrm{ros})_{\max}$, being on par with the standardised form of Byram's (1959) fireline intensity, $I_{\mathrm{Byr}}/I_{\mathrm{Byr,max}}$ with $I_{\mathrm{Byr}} = I \times \Delta x = H_{\mathrm{fc}} \times \Delta w \times \mathrm{ros}$ (in $\mathrm{W\,m^{-1}}$). Insertion of Eqns 17 and 20 shows that $I/I_{\max}$ is a function of wind speed, fuel dryness, and fuel-bed descriptors (Fig. 4).

Besides individual settings of class boundaries, standardised intensities $I/I_{\max}$ can be easily transformed into a user-defined five-class danger rating, e.g. $i = (1, \ldots, 5) = 1 + \mathrm{int}\{5 \times (I/I_{\max})^{a}\}$, with $a = 1$ for a regular class range in $I/I_{\max}$, and $a < 1$ for a non-linear one with small class ranges at small $I/I_{\max}$ ratios. Lower class boundaries are at $I/I_{\max} = \{(i-1)/5\}^{1/a}$. A subjective placement of fire-danger classes on the $I/I_{\max}$ continuum can be done on the basis of prior grassland-fire reports published by environmental agencies or documented in the web and newspaper

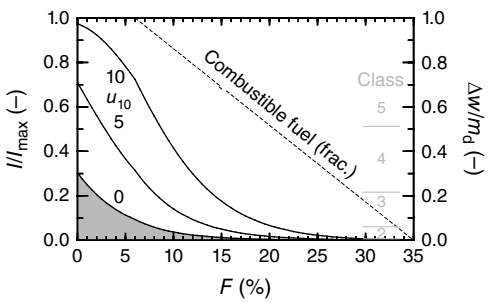

Fig. 4. Standardised fire intensity depending on fuel moisture for 10 m wind speeds of 0, 5, and 10 m s^{-1} (solid curves). Note that in the grey area fire-danger rating is uncertain (e.g. fire intensity in still air tends to zero when ros formula of Cheney *et al.* (1998) is used). The dashed line represents the fractional amount of combustible fuel. Fire-danger class boundaries are exemplarily set at $a = 1/3$ (see text).

(NOAA-National Weather Service (2023)). Standardisation of fire intensity makes the GLFI a relative, dimensionless measure, which facilitates the comparison with other relative fire-danger indices such as the FWI.

Ease-of-ignition index

The dimensionless ease-of-ignition index Q_{ig} indicates the effectiveness of ignition agents releasing different amounts of energy to ignite dead grass at a given moisture content. The formula is based on the minimum energy required to dry out the fuel and raise its initial temperature to ignition temperature before combustion as a self-sustained exothermic reaction can start, i.e.

$$Q_{\mathrm{ig}} = \min\left[\max\left\{\frac{\lambda_{\mathrm{pi}}(F_{\mathrm{up}}, T_{\mathrm{c}}) - \lambda_{\mathrm{pi}}(F, T_{\mathrm{c}})}{\lambda_{\mathrm{pi}}(F_{\mathrm{up}}, T_{\mathrm{c}}) - \lambda_{\mathrm{pi}}(F_{\mathrm{low}}, T_{\mathrm{c}})}, 0\right\}, 1\right] \qquad (22)$$

with λ_{pi} the heat of pre-ignition, F_{up} (44%) the threshold up to which a powerful ignition agent (e.g. a camp fire) is barely able to ignite moist dead grass, and F_{low} (6%) the lower moisture content up to which ignition agents such as small embers and hot particles (Cheney and Sullivan 1997) or minute smouldering firebrands (Cheney 1981) have a high chance of igniting dry grass and result in total fuel combustion.

Following Schroeder (1969), the $\lambda_{\mathrm{pi}}(F, T_{\mathrm{c}})$-formula reads:

$$\begin{aligned}\lambda_{\mathrm{pi}} = {} & (T_{\mathrm{ig}} - T_{\mathrm{c}}) \times (1.89075 + 0.0024283 \times T_{\mathrm{c}}) \\ & + (418.68 - 4.1868 \times T_{\mathrm{c}}) \times F \\ & + 77.60844\{1 - \exp(-15.1 \times F)\} \\ & + 2260.872 \times F \end{aligned} \qquad (23)$$

with λ_{pi} in kJ kg^{-1}, T_{ig} the fuel-specific ignition temperature set at 300°C, which is near 292°C found by von Deichmann (1958) for grass, T_{c} the initial fuel temperature (in °C), and F the fractional moisture content. It is evident that moister and cooler fuels require more energy to start flaming combustion than drier and warmer ones. Consequently, λ_{pi} rises with increasing F and decreasing T_{c}.

The Q_{ig}-function scales the ignition power into the range 0–1 ('ignition unlikely'–'ignition likely'), making Q_{ig} similar to the linear 'ignition potential (IP)' index proposed by Chuvieco *et al.* (2004). The F_{up} threshold given above is a result of extrapolating Chuvieco's linear IP(F) function (defined between IP(0%) = 1.0 and IP(35%) = 0.2, see Discussion) towards IP = 0 giving $F_{\mathrm{up}} = 43.75\%$. A similar value is received based on data of a laboratory 30 s gas-flame ignition experiment (see Electronic Supplement) assuming $F_{\mathrm{up}} = F_{\mathrm{low}} + \Delta p_{\mathrm{ig}} \times (\{\partial p_{\mathrm{ig}}/\partial F\}_{\mathrm{F50}})^{-1} = 6 + 1 \times 38.4 = 44.4\%$, where p_{ig} is the fractional ignition probability and $\{\partial p_{\mathrm{ig}}/\partial F\}_{\mathrm{F50}}$ is the slope of the curve $p_{\mathrm{ig}}(F) = \{1 + \exp(a + b \times F)\}^{-1}$ taken at the 50%-probability of success moisture for sustained ignitions, $F_{50} = F(p_{\mathrm{ig}} = 0.5) = -a/b$.

Model testing: data acquisition

Comparative measurements were conducted at the DWD's Agrometeorological Research Centre located in the northwestern outskirts of Braunschweig ($\lambda = 10°26'55''$E, $\phi = 52°17'35''$N) in northern Germany to test the model performance. We confine our study to lysimetric fuel-moisture measurements and only one outdoor fire experiment because, with rare exceptions, it is illegal to light fires in Germany on the field scale.

Meteorological and fuel-moisture data

To calculate the energy balance and water budget of a grass layer throughout the diurnal cycle, the model needs hourly data consisting of dry and wet-bulb air temperature taken at 2 m standard screen-height level, wind speed at 2 and 10 m (standard anemometer level), down-welling short- and longwave radiation, and precipitation. These data were routinely measured by an automatic weather station installed over a short-grassed meadow in the climate garden of the research centre. With respect to sensor installation heights and sensor accuracies, the measurements fulfilled the WMO (World Meteorological Organization) standards for synoptic measuring networks as documented by WMO (2008).

Total weight of dead grass, m_t, was measured gravimetrically at 15-min intervals covering measuring campaigns of 10 days in August 2009 and 4 weeks in September/October 2015 (see Figs 5 and 6). For this purpose, an electronic balance was used (accuracy: ±0.1 g), part of a self-manufactured mini-lysimeter installed in the upper soil of the climate garden (Wittich 2005). The tray consisted of a metal frame (dimension: $l \times w \times h = 31.7$ cm × 31.4 cm × 4.0 cm) with a wire mesh at its bottom that carried horizontally layered leaves of grass and allowed infiltrated rain water to drain off (discharge not recorded). The grass sample was covered by a coarse-meshed wire net to avoid leaf blow-out due to wind impact. The leaves were clipped 2–6 weeks before the start of the experiments and were stored in the laboratory in the meantime. At the end of the measuring period, the sample was oven-dried in the laboratory at 105°C for 24 h and re-weighed to obtain m_d and $F(t)$.

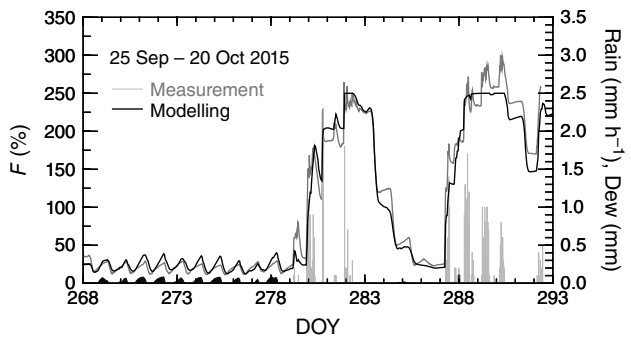

Fig. 5. Moisture content of dead leaves of grass horizontally layered in the wire basket of the mini-lysimeter (grey curve), and analogue modelling (black curve). Vertical grey bars represent precipitation rate, black patches on the abscissa in the radiation nights represent dew events calculated by the model (Braunschweig, 25.9.–20.10.2015, DOY 268–293). Model performance measures: see text.

Outdoor flammability experiment

Experimental burning was conducted around midday of 5 August 2009 (DOY 217, 1240–1320 hours CET (Central European Time)) at the agricultural test site of the DWD station at Braunschweig. For this purpose, two freshly harvested test plots of rye and barley were selected. They were 12×33 m^2 and 40×25 m^2 in area and were covered with residues of clipped straw horizontally layered on standing stubbles (fuel height measured with a rule: about 0.25 m, number of replicates undocumented). The fuel load was estimated as 0.65 kg m^{-2}, and the fuel moisture of both plots measured by oven-drying in the laboratory, was 10.7 and 10.9% (one sample per plot, respectively). The fire was lit by a gas lighter at different spots along the windward field edges. The rate of spread was estimated by measuring elapsed time when the flame front passed metal rods positioned at 5 m intervals in the main wind direction. At 1300 hours CET, under partially cloudy sky, the screen-level air temperature, relative humidity and global radiation were 23.7°C, 35.9%, and 678 W m^{-2}, respectively, and wind speed was at an interim minimum of 1.1 m s^{-1} at 10 m. The measured or calculated time series of weather conditions (Fig. 6*a*, *b*), fuel moisture (Fig. 6*c*, *d*) and fire behaviour (Fig. 6*e*, *f*) extend over a 10-day period centred around the flammability experiment (marked by a vertical arrow). Burning duration of rye and barley plots was between 3 and 5 min and maximum flame height was estimated at 2–3 m.

Results

Fuel-moisture measurements and modelling

Field trials with the lysimeter were conducted in autumn 2015 (25 September–20 October 2015, DOY 268–293) under a broad spectrum of impacting weather conditions that resulted in an *F*-range between 12 and 250–300%. The upper value occurred during and after prolonged periods of rainfall (see Fig. 5), when seepage water probably stagnated in the densely packed tray containing horizontally layered blades of cured grass with an extreme fuel load of 1.2 kg m^{-2}.

During rain-free days, grass moisture exhibits its typical diurnal oscillation: in the evening, water is taken up via adsorption, and at night, dew forms on the canopy surface as the result of strong radiative cooling. Simulated *external dew water* reached a maximum depth of 0.08 mm (m_e =

0.08 kg m^{-2}) on the litter elements (indicated by black patches on the abscissa of Fig. 5), whereas *atmospheric dewfall*, totalled over negative E periods (not shown), accumulated to 0.28 mm, a magnitude in line with nocturnal dew amounts reported by Sudmeyer *et al.* (1994); see also Dawson and Goldsmith (2018) for the significance of dew in Central Europe. The discrepancy of 0.20 mm is due to the transfer of external dew into internal water, which keeps m_e at a low level. During daytime, especially under dry, sunny and windy weather conditions, the nocturnal dew film evaporated and the grass sample lost internal moisture via desorption, yielding diurnal cycles of litter moisture in the range of 12–40%. From DOY 279 onwards (6 October) heavy rainfall resulted in a sharp fuel-moisture increase up to the saturation limit of 250%. After the end of the rainy period (DOY = 282), it took about three dry days to return to the ignition-sensitive moisture range of below ~35% (DOY = 285).

The fuel-moisture model was initialised on 1 January 2015, 0100 hours CET, with initial settings of $F = 250\%$ and $T_c = T_a$, and run under real atmospheric forcing with hourly time steps until 20 October 2015, covering the previous 4-week lysimeter-based fuel-moisture measuring period. Model performance measures show that our calculations are consistent with the observed drying and wetting periods of the dead grass sample, keeping the full moisture range (0–250%) in mind (mean fractional error MFE = $n^{-1}\Sigma|(o_i - c_i)/o_i| =$ 16.7%; mean bias = 3.4%; modified coefficient of efficiency $CE_{mod} = 1 - \{\Sigma|(o_i - c_i)|\}/\{\Sigma|(o_i - o_{av})|\} = 0.87$, with o_i and c_i the observed and calculated variables, respectively, subscript av for average; $CE_{mod} > 0$ indicates reliable model results whereas$CE_{mod} = 1$ is the perfect fit; $CE_{mod} < 0$ suggests a revision of the model according to Legates and McCabe (1999)).

Outdoor flammability experiment and comparison with GFM and FWI model

The following 10-day time series illustrate the weather conditions around the day of the experiment (5 August 2009, DOY 217), along with fuel-moisture outputs of the GLFI and Wotton's GFM model, GLFI's fire-behaviour elements, and Fosberg's Fire Weather Index. The models were initiated on 1 January 2009, 0001 hours CET.

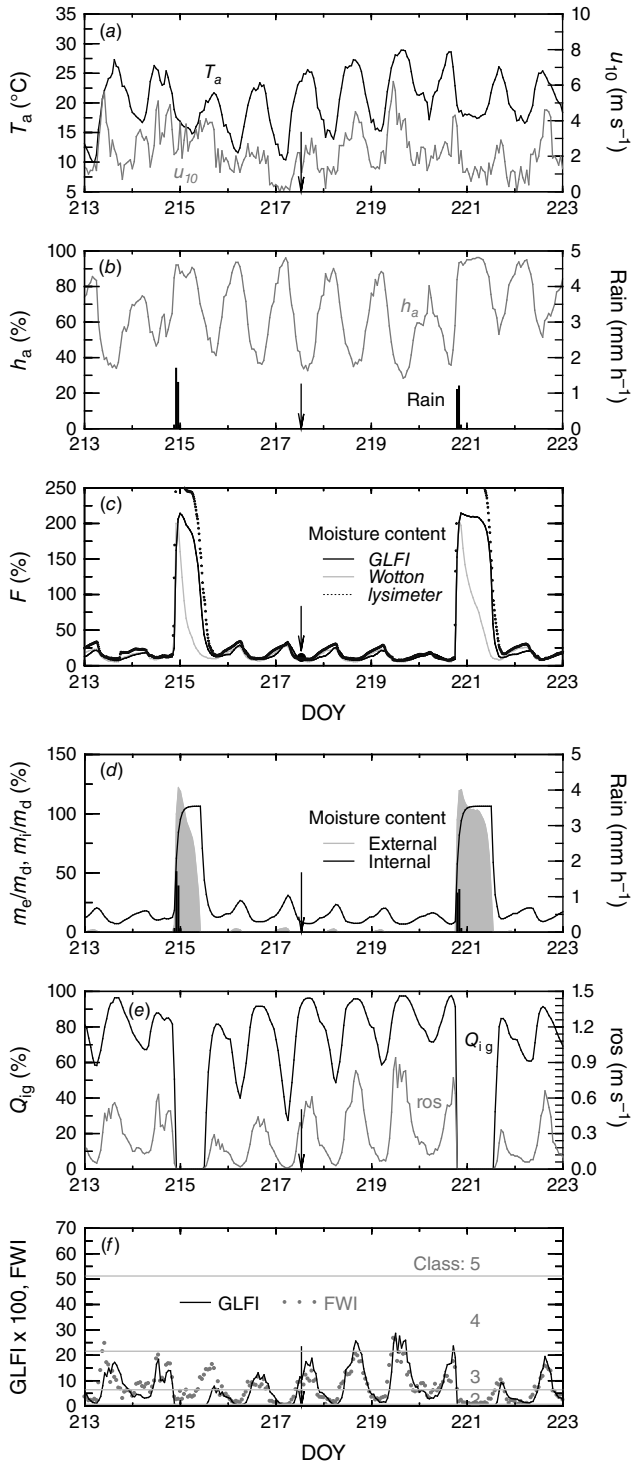

Fig. 6. Hourly weather and fire conditions during the period of 1–11 August 2009 (DOY 213–DOY 223) at DWD-Braunschweig. Around noon on 5 August 2009 (DOY 217, 1240–1320 hours CET (Central European Time), indicated by a vertical arrow), two test fires were lit on a rye and an adjacent spring-barley plot. (*a*) Air temperature at standard measuring level 2 m, T_a, and wind speed at 10 m, u_{10}. (*b*) Relative humidity at 2 m, h_a, and rate of precipitation (bars). (*c*) Grass-moisture content, F, calculated by the GLFI (black curve) and Wotton's GFM model (grey curve), compared with measurements (grain residues, solid circle; cured grass bed in the lysimeter, dotted curve). (*d*) Modelled internal moisture content (black curve) and external moisture content (grey areas with black bars for measured precipitation included), grey patches on the abscissa during rainless periods represent modelled dew events ($m_e/m_d > 0$). (*e*) Normalised ignition indicator, Q_{ig}, and rate of spread, *ros*. (*f*) Standardised intensity (line) with GLFI danger classes and Fosberg's FWI (dots).

During the experiment, at 1240–1320 hours CET, the GLFI yielded a fuel moisture of 8.4% at 1300 hours CET, which is below the crop-residue moisture (10.8%, marked by a black circle in Fig. 6*c*) and the value measured by the grass-carrying mini-lysimeter (9.4%, dotted time series). The GLFI-based fuel-moisture time series is similar to the lysimeter measurement and the GFM modelling (6.5% at 1300 hours CET) for cured matted grass. The GFM model is well suited for comparison because some of its parameters (e.g. $F_{max} = 250\%$, $z_c = 0.3$ m) are near those used in our experiment, but his m_d ($=0.3\,kg\,m^{-2}$) is half that of ours. To attenuate Wotton's calculated daytime grass temperature, which was based on an empirical $S_{\downarrow}$- and u_{10}-dependent formula, his T_c was cut off at $T_a + 10$°C when the difference $T_c - T_a = 10$°C was exceeded. Otherwise, land-surface temperatures of more than 40°C leading to very low fuel moistures of 3% would have been possible. A similar adjustment was necessary in the GLFI model using the $m_{e,max}$-relationship of Menzel (1997) instead of the one by Putuhena and Cordery (1996) to bring computed $F(t)$ time series more in line with Wotton's model results and lysimetric measurements during rain periods. A model comparison of GLFI- versus GFM outputs based on the 10-day time series results in an MFE of 23%. Main differences between both model runs occur during rain periods and at night mainly due to the slightly easier treatment of the nocturnal phase in the GFM model by setting $T_c = T_a$. Comparison with the lysimeter data of Fig. 6*c* provides $E_{mod} = 0.76$ (GFLI) and $E_{mod} = 0.52$ (GFM), so that both models are suitable to reproduce the main features of measured times series.

The Q_{ig} curve in Fig. 6*e* represents the range of ignition success of different agents ($Q_{ig} = 0$: fuel is too moist ($F \geq 44\%$) to be lit by a powerful agent, $Q_{ig} = 1$: fuel is dry enough ($F \leq 6\%$) to be lit by a broad spectrum of agents). As expected, the Q_{ig} time series is reversed to the diurnal fuel-moisture variation (Fig. 6*c*, *d*), reaching 96% at 1300 hours CET on the experimental day after starting at 27% around sunrise because of dew formation in the preceding night.

The calculated fire behaviour at noon on the experiment day was akin to the observed burning conditions: the modelled fire-line speed was $0.4\,m\,s^{-1}$ and the observed speed was $0.5\,m\,s^{-1}$ (about half of the wind speed at 10 m) (Fig. 6*e*). The GLFI classified the medium fire-weather conditions into danger class three (of five; Fig. 6*f*). Fosberg's FWI was in a similar range, but showed higher values under moist (e.g. nocturnal) conditions (see DOY 215).

Discussion

The purpose of this study is to provide insight into some elements of the GLFI that predicts fire danger on a homogeneously cured grass layer in open flat terrain during dynamic weather situations. Because lighting crop and grass fires are generally banned by legal restrictions in Germany (with rare exceptions), our own validation measurements are confined to only two test fires. Therefore, the GLFI relies on theoretical standards (with experimental background) developed by international fire-meteorological communities.

Fuel moisture

Fuel moisture is a central parameter controlling fire behaviour and all its elements. To demonstrate the performance of our fuel-moisture model we compared the outcomes with (1) recordings of a mini-lysimeter and individual measurements taken during two test fires, and (2) the outcome of Wotton's (2009) GFM model.

The GFM model, which originally was adapted to environmental conditions of Ontario/Canada, is integrated into the GLFI to provide additional background information for DWD's advisory staff to verify the GLFI's fuel moisture outcome. Two model modifications became necessary: (1) cutting off the canopy temperature in the GFM at $T_c = T_a + 10$°C when T_c exceeds the 10°C interval (leading to very low fuel moisture); and (2) preferring the more extreme $m_{e,max}$-relationship of Menzel (1997) in the GLFI to get fuel-moisture peaks during rain similar to those obtained by the GFM model. A striking feature in the GFM model is the rapid recovery rate of grass moisture after rainfall, even in nights when relative humidity exceeds 90%. In contrast, the GLFI keeps nocturnal fuel moisture at a high level as a consequence of dewfall or very low evaporation, resulting in longer periods of leaf wetness. For this reason, the energy-balance equation linked with the water-budget concept is a successful alternative to semi-empirical model assumptions regarding atmospheric water-exchange processes.

Ease-of-ignition index Q_{ig}

The Q_{ig}-index indicates the bandwidth of ignition agents with the capacity to light dead grass at a given moisture content ($Q_{ig} \to 1$: broad spectrum of agents (e.g. sparks to campfires) is able to light relatively dry ($F \leq 6\%$) fuels; $Q_{ig} \to 0$: only powerful agents are able to light relatively moist fuels ($F \sim 44\%$). Because $\lambda_{pi}(F)$ is nearly linear, the fraction within the curly brackets of Eqn 22 can be approximated by $(F_{up} - F)/(F_{up} - F_{low})$. Consequently, Q_{ig} is comparable with the ignition potential (IP) index of Chuvieco *et al.* (2004), which is in the range between 1.0 and 0.2 for $0.0 \leq F \leq F_{ex}$ (35%) and between 0.2 and 0 for $F_{ex} < F \leq F_{h\text{-}max}$ (with $F_{h\text{-}max}$ the local historical maximum).

Flammability tables included in Wright and Beall (1948/1968) confirm the lower and upper F limits of the Q_{ig} [= 0–1] range. The tables show the efficiency of a spectrum of ignition agents (from cigarettes to large slash fires) to ignite the forest-duff top layer (grass not included) at different moisture ranges. The drier the fuel, the higher the ignition success, and the broader the spectrum of agents (with different heat-release rates) that are successful igniters.

Fuel moisture of extinction

Remodelling the Initial Spread Index equation allowed the transformation of the ros formula (Eqn 17) into an F_{ex} approximation (Eqn 18), indicating that F_{ex} ($>c_2 = 31\%$) increases with increasing u_{10} up to $F_{ex} \approx 55\%$ for standing grass. This is consistent with the assumption that, when wind tilts the flames forward, the pre-frontal zone receives more radiant energy necessary to dehydrate moister fuels to an ignitable level (see also Cheney *et al.* (1998) who preset F_{ex} at 20% for $u_{10} \leq 2.8\,m\,s^{-1}$, and 24% for $u_{10} > 2.8\,m\,s^{-1}$ resulting in ros $= 0\,m\,s^{-1}$ if $F \geq F_{ex}$).

According to Chuvieco *et al.* (2004), F_{ex} also flags the limit where the likelihood of fire *starting* dramatically decreases. Similarly, Dimitrakopoulos *et al.* (2010) associated F_{ex} with $p_{ig} = 1\%$, resulting in $F_{ex} = 55\%$.

The dependency of Eqn 18 on fuel-bed descriptors is confirmed by Wilson (1985). His empirical estimate for F_{ex} depends on the total surface area of fuel elements per unit ground area, S. When S is replaced by the leaf-area index, one gets $F_{ex} = 0.25 \times \ln(2 \times \text{LAI})$. For short to tall grass canopies characterised by LAIs of 2.5–5.5 $m^2\,m^{-2}$, F_{ex} amounts to 0.40–0.60, a range confirmed by Zhou *et al.* (2005) for live chaparral fuels (but caused by much more environmental factors and fuel-bed descriptors, incl. ground slope). Our Eqn 18 provides F_{ex} values in a similar range, but fuel-bed parameters (Table 1) for standing grass result in smaller F_{ex} values compared with matted/grazed grass when the same ros_{ex}/ros_{max} ratio is used for both canopy types.

Rate of forward spread

In the GLFI we use the rate-of-spread formula of the Canadian FFBP-System as a formal standard that, as a hybrid of double-exponential and power-law structures, is applicable to many other needle- and leaf-like fuel types. However, with regard to its double-exponential form in u_{10} and the inclusion of maximum propagation speed, ros_{max}, it differs from two principal forms of ros(u) functions: one describes a power-law profile, $ros/ros_{min} = 1 + a \times u_{mf}{}^{b}$, proposed by Rothermel (1972, with u_{mf} the mid-flame wind speed) and by Cheney *et al.* (1998, with u_{10} instead); and the other refers to an exponential profile, $ros/ros_{min} = \exp(c \times u_{10})$, used in McArthur's Mark 5 grassland meter (Noble *et al.* 1980). These two alternative forms include the no-wind rate of spread, ros_{min}, which, in the formulas of Rothermel (1972) and Cheney *et al.* (1998), is near zero, whereas the CFFBP-System and Eqn 17 provide spread rates of about $1\,m\,s^{-1}$ in windless and extremely dry ($F = 0\%$) situations.

Another peculiarity discussed by Beer (1993) is the discontinuity in the exponent b of the power-law function when mid-flame wind speed reaches $u_{mf} = 2.5\,m\,s^{-1}$ (or approx. $5\,m\,s^{-1}$ if u_{mf} is logarithmically scaled up from $z_{mf} = 0.5$ to $z = 10$ m standard level). A similar characteristic wind speed value can be found in the ros(u_{10}) formula of the Canadian FFBP-System (i.e. $u_c = 5.5\,m\,s^{-1}$ in Eqn 17), where the ros(u_{10}) profile changes its curvature and starts to adapt to the ros_{max} plateau (see Cruz *et al.* (2022), fig. 6 at $u_{10} = 20\,km\,h^{-1}$). Cheney *et al.* (1998) fixed u_c at $5\,km\,h^{-1}$ ($1.4\,m\,s^{-1}$), i.e. at the minimum wind speed above which consistently heading fires are observed, associated with a change of the power-law exponent from 1 to 0.84. One of the quintessences of Beer's (1993) discussion of the two principal ros(u) forms is that 'neither a simple power-law nor an exponential' function is able to describe the 'true' rate of fire spread so that we accept the double-exponential form.

Note that the rate-of-spread formula we use does not consider the direct influence of fuel load, fuel height, or fuel porosity, although the ros_{max} coefficients in Table 1 are the result of clearly different (i.e. matted vs standing) fuel-bed structures. A number of fire experiments published in the scientific literature, however, suggest the explicit inclusion of fuel-bed descriptors. For example, Davis (1949) proved on the basis of prairie test fires on dense (lightly grazed) and sparse (more heavily grazed) cured grasslands that the former advance more rapidly and with higher intensity. Similarly, Cheney *et al.* (1993) stated that fires in 'natural undisturbed pastures spread 18% faster than fires in cut (or grazed) pastures', but they added that 'there was no evidence that fuel load had a direct influence on spread rate' (p. 40). Field tests by Cruz *et al.* (2020) showed that fire fronts on unharvested cured wheat crops propagate more rapidly ($ros \approx 2\,m\,s^{-1}$ when $m_d = 0.53\,kg\,m^{-2}$, $z_c = 0.73$ m, $\rho_b = 0.726\,kg\,m^{-3}$) than fires on harvested crops ($ros \approx 1.5\,m\,s^{-1}$, $m_d = 0.21\,kg\,m^{-2}$, $z_c = 0.29$ m, $\rho_b = 0.724\,kg\,m^{-3}$). These findings tally closely with McArthur's Australian Grassland Fire Danger Meter, which takes the fuel load into consideration, resulting in fire-spread rates that are twice as high when m_d has doubled (Noble *et al.* 1980). However, Cruz *et al.* (2018) found a positive correlation between m_d and ros only up to $m_d = 0.3\,kg\,m^{-2}$, and an inverse relationship beyond that value, giving an indication that ros is influenced by fuel-bed structure in a complex manner.

Fire intensity

Dry air masses increase the chance of human-related ignition on cured grass areas during calm periods of fine weather. This situation often arises when a high-pressure area moves slowly over the particular forecast region or remains stationary over it. However, if a *mean* wind-based *low* ros-value is taken as a basis for fire-intensity estimates on sunny days, the danger level may remain underrated when convective heat transport associated with rising thermal plumes, isolated gusts, and increased turbulence (Aylor *et al.* 1993) is ignored (Noble *et al.* 1980). Fluctuating winds result in advective pre-heating of fuels at low wind speeds (Beer 1991) and rapid amplification of pyrolysis (Cheney and Gould 1995). Fire managers evaluate such fire situations as dangerous even if the burnt area per fire incidence remains relatively small. This is the practical reason why we

prefer the Canadian ros formula, which gives higher fire intensities and danger ratings in the range of low wind speeds compared with the formula of Cheney *et al.* (1998). Some consequences can be demonstrated with the example of the *Ossendorf Fire*, which was sparked off during harvesting operations in a grain field near Ossendorf (eastern Germany) in the afternoon of 20 July 2006 (DOY 201). After burning an area of 4 ha, the crop fire ran into the nearby forest and destroyed a further 61 ha of coniferous woods. Weather data were recorded at a distance of approx. 10–30 km from the fire (meteorological stations: Lindenberg, Coschen), providing $h_{a,min}$ = 13.5–18.2%, $T_{a,max}$ = 35.5–36.6°C, and $u_{10,max}$ = 2.5–4.0 m s^{-1}. The last significant rain fell a week before the fire event (in the afternoon and night of 13/14 July, DOY 194/195), totalling 0.5–6.9 mm. On that fire day, based on calculated very low fuel moistures of 4% and ros values of approx. 1 m s^{-1} (Fig. 7*a*, *b*), the GLFI provided a higher danger rating than the FWI, whose afternoon peak was nearly at its minimum in the 10-day time series of Fig. 7*c*. Note that the *Ossendorf Fire* led to a safety recommendation for farmers declaring that, immediately before harvesting, a firebreak has to be ploughed around fields adjacent to forests (Müller 2007).

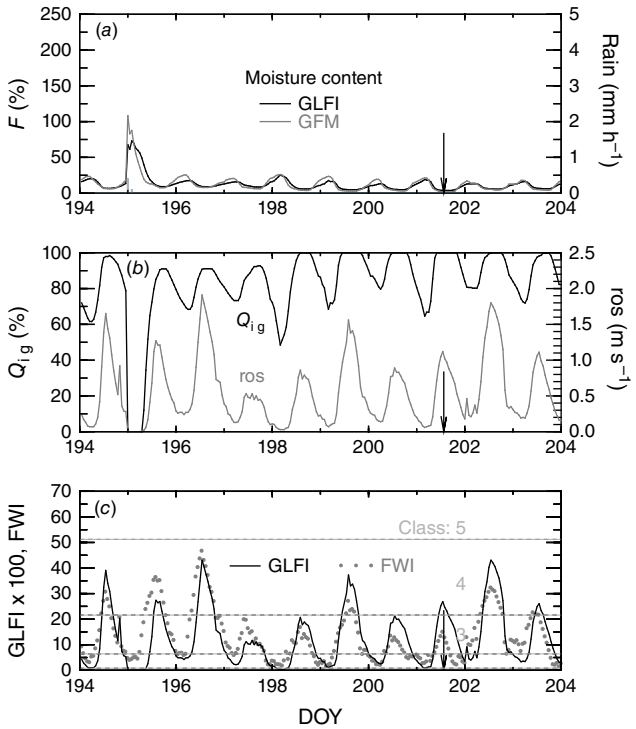

Fig. 7. (*a*) Hourly fuel moisture according to GLFI and GFM models during the period of 13–23 July 2006 (DOY 194–204) at met. station Coschen. (*b*) Normalised ignition indicator (Q_{ig}) and rate of spread (ros). (*c*) GLFI's standardised fire intensity (line) and Fosberg's FWI (dots). The grass fire started in the afternoon of 20 July (DOY 201, indicated by a vertical arrow). (*d*) Aerial photo of the *Ossendorf Fire* spreading from the grain field into the nearby forest, with the absence of an intermittent firebreak (source: Innenministerium Brandenburg).

Fig. 7*c* shows that sinusoidal 24-h-time patterns of GLFI and FWI are similar (MAE = 5.4%), which is to be expected because fire intensity and flame length are positively correlated to each other (Byram 1959; Alexander 1982). Nevertheless, on DOY 194/195 the typical FWI artefact occurred when rain wetted the grain canopy and led to fuel moistures of 70–100%, non-ignitibility and no-spread conditions (Fig. 7*a*, *b*), but the FWI does not zero, and unlike the GLFI, rises immediately after sunrise under still moist conditions due to lacking inertia (no time-lag/memory effect).

Conclusions and outlook

The GLFI model fulfils several demands on modern rating systems:

- It estimates fire danger of cured grass layers on an hourly basis throughout the diurnal cycle;
- It uses meteorological energy-balance and water-budget (i.e. state-of-the art) principles;
- It considers all elements of fuel moisture and different modes of water-transfer processes; and
- It estimates fire behaviour based on standardised fire-reaction intensity, fire-spread rate, and ease-of-ignition measure.

The GLFI's limitations are:

- Overrating fire danger when living grasses can take up soil water via an active root system; and
- Less precise fire-weather forecast at locations distant from meteorological stations (see also Cheney and Gould 1995), and under frost conditions in the cold season.

Model improvement including reliable all-season forecast is achieved by: (1) coupling of a soil-moisture based phenology model that reduces fire risk during periods of greenness; (2) testing the validity of F_{eq} formulas and water-transfer relationships under freeze/thaw conditions and enhancing the predictive accuracy in the winter months when, for example, in the Alpine region foehn-like winds above subsidence inversions raise the fire danger (note that Alexander *et al.* (2013) demonstrated the benefit of grassland fire

prediction in dry and snowless spells of the Canadian cold season); and (3) closure of weather-observation gaps in remote areas via grid-based modelling using countrywide re-analysed meteorological surface data (e.g. full spatial coverage is essential in complex terrain where slope and aspect may significantly affect fuel moisture and rate of fire spread, and where reversed weather situations may occur along the altitudinal gradient when an inversion layer has formed).

Model calibration and experimental validation including traditional fuel-moisture sampling in canopies with standing grasses and smaller fuel loads will be a permanent task. More test fires in the field scale, if possible, will help to verify the fire-behaviour components.

Supplementary material

Supplementary material is available online.

References

Albini FA (1976) Estimating wildfire behaviour and effects. General Technical Report INT-30. (USDA Forest Service, Intermountain Forest and Range Experiment Station: Ogden, UT)

Alexander ME (1982) Calculating and interpreting forest fire intensities. *Canadian Journal of Botany* **60**, 349–357. doi:10.1139/b82-048

Alexander ME, Heathcott MJ, Schwanke RL (2013) 'Fire behaviour case study of two early winter grass fires in southern Alberta, 27 November 2011'. 76 p. (Partners in Protection Association: Edmonton, AB, Canada)

Alfieri JG, Niyogi D, Blanken PD, Chen F, LeMone MA, Mitchell KE, Ek MB, Kumar A (2008) Estimation of the minimum canopy resistance for croplands and grasslands using data from the 2002 International H_2O Project. *Monthly Weather Review* **136**, 4452–4469. doi:10.1175/2008MWR2524.1

Anderson HE (1982) Aids to determining fuel models for estimating fire behaviour. General Technical Report INT-122. (USDA Forest Service, Intermountain Forest and Range Experiment Station: Ogden, UT)

Anderson HE (1990*a*) Predicting equilibrium moisture content of some foliar forest litter in the Northern Rocky Mountains. Research Paper INT-429. (USDA Forest Service, Intermountain Research Station: Ogden, UT)

Anderson HE (1990*b*) Moisture diffusivity and response time in fine forest fuels. *Canadian Journal of Forest Research* **20**, 315–325. doi:10.1139/x90-046

Aylor DE, Wang Y, Miller DR (1993) Intermittent wind close to the ground within a grass canopy. *Boundary-Layer Meteorology* **66**, 427–448. doi:10.1007/BF00712732

Beck JA, Alexander ME, Harvey SD, Beaver AK (2002) Forecasting diurnal variations in fire intensity to enhance wildland firefighter safety. *International Journal of Wildland Fire* **11**, 173–182. doi:10.1071/WF02002

Beer T (1991) The interaction of wind and fire. *Boundary-Layer Meteorology* **54**, 287–308. doi:10.1007/BF00183958

Beer T (1993) The speed of a fire front and its dependence on wind speed. *International Journal of Wildland Fire* **3**, 193–202. doi:10.1071/WF9930193

Breinl K, DiBaldassarre G, Mazzoleni M, Lun D, Vico G (2020) Extreme dry and wet spells face changes in their duration and timing. *Environmental Research Letters* **15**, 074040. doi:10.1088/1748-9326/ab7d05

Byram GM (1959) Combustion of forest fuels. In 'Forest fire: control and use'. (Ed. KP Davis) pp. 61–89. (McGraw-Hill: New York, NY, USA)

Campbell GS (1977) 'An Introduction to Environmental Biophysics.' (Springer Verlag: Heidelberg, Germany)

Catchpole EA, Catchpole WR, Viney NR, McCaw WL, Marsden-Smedley JB (2001) Estimating fuel response time and predicting fuel moisture content from field data. *International Journal of Wildland Fire* **10**, 215–222. doi:10.1071/WF01011

Cheney NP (1981) Fire behaviour. In 'Fire and the Australian biota'. (Eds AM Gill, RH Groves, IR Noble) pp. 151–175. (Australian Academy of Science: Canberra, ACT)

Cheney NP (1990) Quantifying bushfires. Mathematical and Computer Modelling 13, 9–15. doi:10.1016/0895-7177(90)90094-4

Cheney NP, Gould JS (1995) Fire growth in grassland fuels. *International Journal of Wildland Fire* **5**, 237–247. doi:10.1071/WF9950237

Cheney P, Sullivan A (1997) 'Grassfires: fuel, weather and fire behaviour.' (CSIRO Publishing: Melbourne, Australia)

Cheney NP, Gould JS, Catchpole WR (1993) The influence of fuel, weather and fire shape variables on fire-spread in grasslands. *International Journal of Wildland Fire* **3**, 31–44. doi:10.1071/WF9930031

Cheney NP, Gould JS, Catchpole WR (1998) Prediction of fire spread in grasslands. *International Journal of Wildland Fire* **8**, 1–13. doi:10.1071/WF9980001

Choudhury BJ, Reginato RJ, Idso SB (1986) An analysis of infrared temperature observations over wheat and calculation of latent heat flux. *Agricultural and Forest Meteorology* **37**, 75–88. doi:10.1016/0168-1923(86)90029-8

Chuvieco E, Aguado I, Dimitrakopoulos AP (2004) Conversion of fuel moisture content values to ignition potential for integrated fire danger assessment. *Canadian Journal of Forest Research* **34**, 2284–2293. doi:10.1139/x04-101

Couturier DE, Ripley EA (1973) Rainfall interception in mixed grass prairie. *Canadian Journal of Plant Science* **53**, 659–663. doi:10.4141/cjps73-130

Cruz MG, Sullivan AL, Gould JS, Hurley RJ, Plucinski MP (2018) Got to burn to learn: the effect of fuel load on grassland fire behaviour and its management implications. *International Journal of Wildland Fire* **27**, 727–741. doi:10.1071/WF18082

Cruz MG, Hurley RJ, Bessell R, Sullivan AL (2020) Fire behaviour in wheat crops – effect of fuel structure on rate of fire spread. *International Journal of Wildland Fire* **29**, 258–271. doi:10.1071/WF19139

Cruz MG, Alexander ME, Kilinc M (2022) Wildfire rates of spread in grasslands under critical burning conditions. *Fire* **5**, 55. doi:10.3390/fire5020055

Davis WS (1949) The rate of spread - fuel density relationship. *Fire Control Notes* **10**(2), 8–9.

Dawson TE, Goldsmith GR (2018) The value of wet leaves. *New Phytologist* **219**, 1156–1169. doi:10.1111/nph.15307

de Groot WJ, Wardati , Wang Y (2005) Calibrating the Fine Fuel Moisture Code for grass ignition potential in Sumatra, Indonesia. *International Journal of Wildland Fire* **14**, 161–168. doi:10.1071/WF04054

Deutscher Wetterdienst (2022) German Climate Atlas 2022. Available at https://www.dwd.de/EN/climate_environment/climateatlas/climateatlas_node.html [verified 1 June 2023]

Dimitrakopoulos AP, Mitsopoulos ID, Gatoulas K (2010) Assessing ignition probability and moisture of extinction in a Mediterranean grass fuel. *International Journal of Wildland Fire* **19**, 29–34. doi:10.1071/WF08124

Forestry Canada Fire Danger Group (1992) Development and Structure of the Canadian Forest Fire Behaviour Prediction System. Forestry Canada, Information Report ST-X-3. (Science and Sustainable Development Directorate: Ottawa, Canada)

Fosberg MA (1978) Weather in wildland fire management: the Fire Weather Index. In 'Proceedings of the Conference on Sierra Nevada Meteorology', 19–21 June 1978, South Lake Tahoe, CA, USA. pp.1–4 (American Meteorological Society: Boston, MA)

Kidnie S, Wotton BM (2015) Characterisation of the fuel and fire environment in southern Ontario's tallgrass prairie. *International Journal of Wildland Fire* **24**, 1118–1128. doi:10.1071/WF14214

Legates DR, McCabe GJ (1999) Evaluating the use of "goodness-of-fit" measures in hydrologic and hydroclimatic model validation. *Water Resources Research* **35**, 233–241. doi:10.1029/1998WR900018

Lex P, Wittich K-P (2002) Begünstigt das Mikroklima an Bahntrassen die Entstehung von Böschungs- und Waldbränden? AFZ-Der Wald 57, 6666-70 [in German].

Liang X, Su D, Yin S, Wang Z (2009) Leaf water absorption and desorption functions for three turfgrasses. *Journal of Hydrology* **376**, 243–248. doi:10.1016/j.jhydrol.2009.07.035

Luke RH, McArthur AG (1978) 'Bushfires in Australia'. Department of Primary Industry, Forestry and Timer Bureau. (CSIRO Division of Forest Research: Canberra, ACT)

Marsden-Smedley JB, Catchpole WR (2001) Fire modelling in Tasmanian buttongrass moorlands. III. Dead fuel moisture. *International Journal of Wildland Fire* **10**, 241–253. doi:10.1071/WF01025

Matthews S (2006) A process-based model of fine fuel moisture. *International Journal of Wildland Fire* **15**, 155–168. doi:10.1071/WF05063

Matthews S (2010) Effect of drying temperature on fuel moisture content measurements. *International Journal of Wildland Fire* **19**, 800–802. doi:10.1071/WF08188

Matthews S (2022) Australian fire danger rating system: Fire behaviour index technical guide. Available at https://www.afac.com.au/initiative/afdrs/article/fire-behaviour-index-technical-guide [verified 1 June 2023]

McArthur AG (1966) Weather and Grassland Fire Behaviour. Commonwealth Department of National Development, Forestry and Timber Bureau Leaflet 100, Canberra, ACT.

McGechan MB, Pitt RE (1990) The rewetting of partially dried grass swaths by rain: Part 2, Exploratory experiments into absorption and drying rates. *Journal of Agricultural Engineering Research* **45**, 69–76. doi:10.1016/S0021-8634(05)80139-8

Menzel L (1997) Modellierung der Evapotranspiration im System Boden-Pflanze-Atmosphäre. Züricher Geographische Schriften 67, Geographisches Institut, ETH Zürich, Switzerland [in German].

Monteith JL (1965) Evaporation and environment. *Symposia of the Society for Experimental Biology* **19**, 205–234.

Müller C (1992) Waldbrandgefährdung und Waldbrandschutz im Land Brandenburg. *Allgemeine Forstzeitschrift* **18**, 973–974.

Müller R (2007) 61 Hektar in 5 Stunden – Analyse und Folgen des Großbrandes. 'Fachtagung zur Bewirtschaftung und Ökologie der Kiefer im nordostdeutschen Tiefland', 15–16 November 2007, Eberswalde, internal paper, 1 p. [In German].

National Wildfire Coordinating Group (2002) Gaining an understanding of the National Fire Danger Rating System. PMS 932, NFES 2665. (National Interagency Fire Center: Boise, ID, USA)

National Wildfire Coordinating Group (2008) Glossary of wildland fire terminology. PMS 205. (National Interagency Fire Center: Boise, ID, USA)

Nelson Jr RM (1983) A model for sorption of water vapor by cellulosic materials. *Wood and Fiber Science* **15**, 8–22.

NOAA-National Weather Service (2023) Glossary of fire weather terms. Available at https://www.weather.gov./phi/fire_glossary [verified 1 June 2023]

Noble JC (1991) Behaviour of a very fast grassland wildfire on the Riverine Plain of southeastern Australia. *International Journal of Wildland Fire* **1**, 189–196. doi:10.1071/WF9910189

Noble IR, Bary GAV, Gill AM (1980) McArthur's fire-danger meters expressed as equations. *Australian Journal of Ecology* **5**, 201–203. doi:10.1111/j.1442-9993.1980.tb01243.x

Putuhena WM, Cordery I (1996) Estimation of interception capacity of the forest floor. *Journal of Hydrology* **180**, 283–299. doi:10.1016/0022-1694(95)02883-8

Rothermel RC (1972) A mathematical model for predicting fire spread in wildland fuels. Research Paper INT-115 (USDA Forest Service, Intermountain Forest and Range Experiment Station: Ogden, UT)

Schroeder MJ (1969) Ignition probability. Office Report 2106-1. USDA Forest Service, Rocky Mountain Forest and Range Experiment Station.

Sharples JJ (2009) An overview of mountain meteorological effects relevant to fire behaviour and bushfire risk. *International Journal of Wildland Fire* **18**, 737–754. doi:10.1071/WF08041

Sneeuwjagt RJ, Frandsen WH (1977) Behavior of experimental grass fires vs. predictions based on Rothermel's fire model. *Canadian Journal of Forest Research* **7**, 357–367. doi:10.1139/x77-045

Sudmeyer RA, Nulsen RA, Scott WD (1994) Measured dewfall and potential condensation on grazed pasture in the Collie River basin, southwestern Australia. *Journal of Hydrology* **154**, 255–269. doi:10.1016/0022-1694(94)90220-8

Sutherland RA (1986) Broadband and spectral emissivities (2–18 μm) of some natural soils and vegetation. *Journal of Atmospheric and Oceanic Technology* **3**, 199–202. doi:10.1175/1520-0426(1986)003<0199:BASEOS>2.0.CO;2

Thompson N (1981) Modelling the field drying of hay. *The Journal of Agricultural Science* **97**, 241–260. doi:10.1017/S0021859600040685

Van Wagner CE (1972) Equilibrium moisture contents of some fine forest fuels in eastern Canada. Information Report PS-X-36. (Canadian Forestry Service, Petawawa Forest Experiment Station)

Vegas Galdos F, Álvarez C, García A, Revilla JA (2012) Estimated distributed rainfall interception using a simple conceptual model and Moderate Resolution Imaging Spectroradiometer (MODIS). *Journal of Hydrology* **468–469**, 213–228. doi:10.1016/j.jhydrol.2012.08.043

von Deichmann V (1958) Untersuchungen über die Entzündlichkeit und Brennbarkeit von Bodendecken als Beitrag zu den Grundlagen einer Waldbrandprognose. Dissertation, Forstliche Fakultät, Georg-August-Universität Göttingen, Germany [In German].

Wilson Jr RA (1985) Observations of extinction and marginal burning states in free burning porous fuel beds. *Combustion Science and Technology* **44**, 179–193. doi:10.1080/00102208508960302

Wilson Jr RA (1990) Reexamination of Rothermel's fire spread equations in no-wind and no-slope conditions. Research Paper INT-434. (USDA Forest Service, Intermountain Research Station: Ogden, UT)

Wittich K-P (2005) A single-layer litter-moisture model for estimating forest-fire danger. *Meteorologische Zeitschrift* **14**, 157–164. doi:10.1127/0941-2948/2005/0017

WMO (2008) 'Guide to Meteorological Instruments and Methods of Observation. WMO-No. 8, Vol. 1, Measurement of Meteorological Variables.' (World Meteorological Organization: Geneva) Available at https://www.weather.gov/media/epz/mesonet/CWOP-WMO8.pdf [verified 1 June 2023]

Wotton BM (2009) A grass moisture model for the Canadian Forest Fire Danger Rating System. In 'Proceedings 8th Symposium on Fire and Forest Meteorology', Kalispell MT, 13–15 October 2009. Paper 3A.2. (American Meteorological Society)

Wright JG, Beall HW (1945/1968) The application of meteorology to forest fire protection. Technical Communication No. 4. Imperial Forestry Bureau, Oxford. Information Report FF-X-11. (Reprinted by Forest Fire Research Institute, Department of Forestry and Rural Development: Ottawa, Canada)

Zhou X, Mahalingam S, Weise D (2005) Modeling of marginal burning state of fire spread in live chaparral shrub fuel bed. *Combustion and Flame* **143**, 183–198. doi:10.1016/j.combustflame.2005.05.013

Zolina O, Simmer C, Belyaev K, Gulev SK, Koltermann P (2013) Changes in the duration of European wet and dry spells during the last 60 years. *Journal of Climate* **26**, 2022–2047. doi:10.1175/JCLI-D-11-00498.1

Data availability. Data will be shared upon reasonable request to the corresponding author.

Conflicts of interest. The authors declare no conflicts of interest.

Declaration of funding. This research did not receive any specific funding.

Author affiliation
[A]Deutscher Wetterdienst (German Meteorological Service), Centre for Agrometeorological Research, Bundesallee 33, D-38116 Braunschweig, Germany.